# Energetic Basis of Human Telomeric DNA Folding into G-Quadruplex Structures

Matjaž Bončina, Jurij Lah,* Iztok Prislan, and Gorazd Vesnaver*

Faculty of Chemistry and Chemical Technology, University of Ljubljana, SI−1000 Ljubljana, Slovenia

Ⓢ *Supporting Information*

ABSTRACT: Recent theoretical studies performed on the folding/ unfolding mechanism of the model telomeric human DNA, 5′- AGGGTTAGGGTTAGGGTTAGGG-3′ (Tel22), have indicated that in the presence of K^+ ions Tel22 folds into two hybrid G- quadruplex structures characterized by one double and two reversal TTA loops arranged in a different way. They predicted a new unfolding pathway from the initial mixture of hybrid G-quadruplexes via the corresponding intermediate triplex structures into the final, fully unfolded state. Significantly, no experimental evidence supporting the suggested pathway has been reported. In the current

work, we performed a comprehensive global thermodynamic analysis of calorimetric (DSC, ITC) and spectroscopic (CD) data obtained on monitoring the folding/unfolding of Tel22 induced by changes of temperature and K^+ concentration. We show that unfolding of Tel22 may be described as a monomolecular equilibrium three-state process that involves thermodynamically distinguishable folded (F), intermediate (I), and unfolded (U) state. Considering that calorimetric methods cannot distinguish between energetically similar G-quadruplex or triplex conformations predicted by the theoretical model one can conclude that our results represent the first experimental support of the suggested unfolding/folding mechanism of Tel22. This conclusion is confirmed by the fact that the estimated number of K^+ ions released upon each unfolding step in our thermodynamic model agrees well with the corresponding values predicted by the theoretical model and that the observed changes in enthalpy, entropy, and heat capacity accompanying the F → I and I → U transitions can be reasonably explained only if the intermediate state I is considered to be a triplex structural conformation.
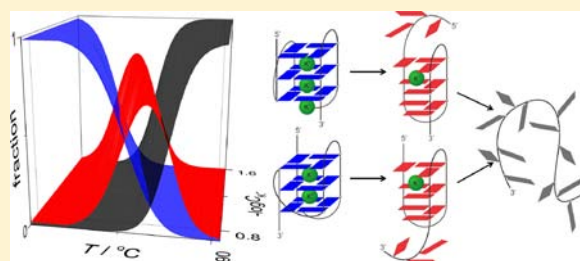
■ INTRODUCTION

It is well-known that guanine-rich DNA sequences can form complex structures called G-quadruplexes in which four guanines are held in plane with eight Hoogsteen hydrogen bonds and are additionally stabilized with stacking interactions between the neighboring G-quartets.[1] Such G-quadruplex structures require cations for their formation. Depending on their size, cations are localized between the two G-quartets or within the plane of G-quartet and form coordination bonds with the carbonyl oxygen of guanines. It is now well established that sequence details and the nature of the ion play a crucial role in the structure stability and structural diversity of G- quadruplexes.[2−12] In general, G-quadruplexes may be formed via intramolecular folding (monomolecular) and by association of two (bimolecular) or four (tetramolecular) DNA chains. According to the mutual orientations of the core segments of DNA, the G-quadruplex structure can be further arranged into parallel or anti-parallel configuration. Also possible are so-called hybrid structures in which the orientation of guanine segments is neither fully parallel nor anti-parallel.[8,13−15] Overall, the existing data on G-quadruplex structures reveal that no simple correlation has emerged among their structural diversity and the molecularity, strand polarity, guanine glycosidic conforma- tion, and the nature of the cations.

Numerous investigations have shown that G-quadruplexes can be formed in the G-rich regions of telomeric DNA which by capping the ends of linear chromosomes prevents recombination and fusion of different parts of the DNA chains and/or degradation of DNA by the action of nucleases. In humans, telomers consist of tandem repeats of d(TTAGGG) for 5−8 kb in length structured in double helical form. They terminate in single chain 3′-overhangs of 100−200 bases in length. The telomere serves as a biological clock since in normal cells each cell replication is accompanied by a 50−200 base loss of the telomere and such progressive decrease in length eventually leads to the cell apoptosis. Telomers of the cancer cells, however, do not shorten on replication and in 85− 90% of human cancer cells increased activity of the enzyme telomerase which prevents such shortening has been detected. Moreover, the formation of stable G-quadruplexes in the region of the telomeric single-stranded overhangs has been found to inhibit telomerase activity.[16−19] Therefore, telomeric G- quadruplexes are emerging as promising targets for anticancer agents able to inhibit the telomerase activity by binding to G- quadruplexes and thus stabilizing them.[20−22] Evidently, successful anticancer ligands used in such interventions should

exhibit an exquisite specificity for G-quadruplexes over duplexes and ability to discriminate one G-quadruplex over the other.[23,24] In attempting to find such ligands, understanding the driving forces that determine the stability and folding pathways of G-quadruplex structures and their dependence on the solution conditions (temperature, cation type) and the type of the ligand undoubtedly plays a crucial role.[12,25−27]

Despite tremendous progress in understanding of G-quadruplexes made over the last years, there are still many unanswered questions concerning their biological role, formation, structure, and physicochemical properties. In this context, X-ray crystallography and NMR spectroscopy can provide important structural information. However, attempts to investigate the G-quadruplex structures in a solution as a function of temperature and salt type (Na$^+$, K$^+$) by these two techniques may lead to contradictory results.[28−30] Thus, X-ray crystallography shows that sequence 5′-AGGGTTAGGGT-TAGGGTTAGGG-3′ (Tel22) in the presence of K$^+$ ions adopts a propeller-type structure in which four parallel strands are connected with three external loops.[28] By contrast, NMR and some biophysical techniques indicate that in K$^+$ solutions at room temperature, Tel22 exists as a mixture of unknown topologies.[14,31,32] Recently, Chaires et al. have suggested, based on NMR, fluorescence, CD experiments, and molecular modeling, that Tel22 in K$^+$ solutions appears as an equilibrium mixture of two (3 + 1) hybrid-type G-quadruplex structures, Hybrid-1 and Hybrid-2.[33] Their molecular dynamics simulations also suggest that in addition to two channel K$^+$-binding sites existing in both hybrid structures, the Hybid-1 conformation contains one external coordination K$^+$-binding site capable of specific binding of an additional K$^+$ ion. Similar results were reported also by Sugiyama et al. in their recent study of folding pathways of Tel22 in K$^+$ solutions. On the basis of ab initio molecular dynamics and fragment molecular orbital calculations, they propose that the Hybrid-1 and Hybrid-2 G-quadruplex structures are formed through corresponding intermediate triplex structures that contain only one channel K$^+$-binding site.[34]

It has been widely recognized that the polymorphism and conformational transitions of G-quadruplexes can also be studied using biophysical experimental techniques such as UV absorption and CD spectroscopy, differential scanning calorimetry (DSC), isothermal titration calorimetry (ITC), and gel electrophoresis. Using these methods, we attempted in the present work to investigate the mechanism and driving forces of Tel22 folding/unfolding in K$^+$ solutions. The corresponding temperature and K$^+$ concentration dependent calorimetric and spectroscopic data were successfully described in terms of an equilibrium model mechanism, suggesting coexistence and interconversion of three monomolecular Tel22 conformations: a fully folded G-quadruplex, an intermediate partially unfolded G-quadruplex (triplex) and a fully unfolded single-stranded form (Figure 1). We demonstrate that the obtained thermodynamic driving forces of Tel22 folding/unfolding are in accordance with the results reported recently by Chaires et al.[33] and support the mechanism of Tel22 folding suggested by Sugiyama et al.[34]

■ MATERIALS AND METHODS

Sample Preparation. Oligonucleotide 5′-AGGGT-TAGGGTTAGGGTTAGGG-3′ (Tel22) was obtained HPLC pure from Midland Co., U.S. The buffer solutions used in our experiments consisted of 20 mM cacodylic acid (DSC, CD,
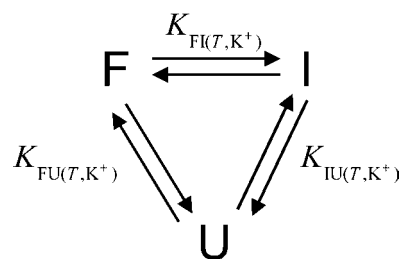
Figure 1. Proposed equilibrium three-state model for the thermally induced folding/unfolding of Tel22 that assumes coexistence and interconversion of intramolecular G-quadruplex structure F, an intermediate partially unfolded G-quadruplex (triplex) structure I and an unfolded structure U.

UV) or 20 mM TRIS (ITC), 1 mM EDTA, and various concentrations of K$^+$ ions. KOH was added to cacodylic acid or HCl to TRIS to reach pH = 6.9. Then, KCl was added to obtain the desired concentration of K$^+$ ions (25, 70 in 200 mM K$^+$ in cacodylic buffer and 8 mM K$^+$ in TRIS buffer). DNA was first dissolved in water and then extensively dialyzed against the buffer (three changes of buffer solutions in 24 h) using a dialysis tube Float-A-Lyser (Spectrum Laboratories, U.S., M_w cutoff 500 Da). Concentration of the DNA in the buffer solution was determined spectrophotometrically at 25 °C. For the extinction coefficient of their single-stranded forms at 25 °C we used the value ε_{260} = 228 500 M^{-1}cm^{-1} estimated from the nearest-neighbor data of Cantor et al.[35] The starting solution of oligonucleotide was first heated to 95 °C in an outer thermostat for 5 min to make sure that all of the DNA transforms into the unfolded form, then cooled to 5 °C at the cooling rate of 0.05 °C/min to allow DNA to adopt quadruplex structure(s), and then used in the DSC, CD, UV, or ITC experiments.

UV Melting Experiments. Absorbance versus temperature profiles of DNA samples were measured in a Cary 100 BIO UV−vis Spectrophotometer (Varian Inc.) equipped with a thermoelectric temperature controller using cells of 0.25 mm path length. Melting of Tel22 G-quadruplexes ($c_{DNA} \approx 0.5$ mM in single strands) at the heating rate of 1.0 °C/min followed by their formation at the cooling rate of 1.0 °C/min was monitored at 260 and 293 nm between 5 and 95 °C. Accurate concentrations at 25 °C were obtained from the melting curves monitored at 260 nm.[36] The dependence of Tel22 melting transitions in K$^+$ solutions on the DNA concentration was followed by UV melting curves measured at λ = 293 nm.

Differential Scanning Calorimetry (DSC). DSC experiments were performed using Nano DSC instrument (TA Instruments, New Castle, DE, U.S.). The G-quadruplex concentration used in these DSC studies was about 0.5 mM in single strands. Cyclic DSC measurements were performed at the heating and cooling rates of 0.5, 1.0, and 2.0 °C/min. The measured temperature interval was between 1 and 95 °C. The corresponding baseline (buffer−buffer) scans were subtracted from the unfolding/folding scans and normalized to 1 mol of G-quadruplex in single strands to obtain partial molar heat capacity of DNA, $\bar{C}_{P,2}$, as a function of temperature.

CD Spectroscopy. CD spectra of the G-quadruplexes were measured as a function of temperature in an AVIV CD Spectrophotometer 62A DS (Aviv Biomedical, Lakewood, NJ, U.S.) equipped with a thermoelectric temperature controller. Ellipticity, θ, was measured between 5 and 95 °C in the temperature intervals of 1 °C at different heating rates. CD spectra of samples ($c_{DNA} \approx 0.5$ mM in single strands) were

collected between 215 and 320 nm in a 0.25 mm cuvette with a signal averaging time of 10 s and 5 nm bandwidth. The thermally induced unfolding of Tel22 quadruplexes was followed at different K^+ concentrations by CD melting curves measured at λ = 265 and 293 nm. To check for the concentration dependence of the observed melting transitions, the CD melting curves were measured also at several DNA concentrations between 0.03 and 0.5 mM.

Isothermal Titration Calorimetry (ITC). ITC experiments were performed on sample ($c_{DNA} \approx 0.3$ mM in single strands, TRIS buffer, 8 mM in K^+) and the corresponding blank solution at 5 °C using a VP-ITC isothermal titration calorimeter (Microcal Inc., Northampton, MA, U.S.). TRIS buffer solution containing 40 mM KCl was added stepwise (ΔV = 5 μL) to the sample or blank solution and the accompanying enthalpy changes, expressed per mole of added KCl per injection, were obtained from the area under the measured peaks.

■ RESULTS AND DISCUSSION

Folding/Unfolding As a Three-State Process. To check the possible effect of kinetics on polymorphism and conformational transitions of G-quadruplexes, samples were placed in a hot bath (95 °C) for 5 min and then cooled down at slow (0.05 °C/min) or moderate (0.5 − 2.0 °C/min) cooling rates. In this way prepared G-quadruplexes were characterized by DSC thermograms and CD and UV transition curves monitored at different heating and cooling rates. Our results obtained with two separately purchased and purified Tel22 samples show that at each concentration of K^+ ions the DSC thermograms as well as the CD and UV spectra and the corresponding melting and cooling curves are reproducible and independent of the heating or cooling rates at which they were measured and on the cooling rates at which the DNA samples were prepared. Thus, the folding and unfolding process of human telomeric sequence Tel22 in the presence of K^+ ions may be considered as an equilibrium process, in which, according to the observed independency of the normalized CD and UV melting curves and PAGE experiments on strand concentration (see SI Figures S1, S2) only intramolecular complexes are involved. Furthermore, the shapes of the CD and UV melting curves and DSC thermograms strongly suggest that the thermal unfolding of the Tel22 G-quadruplex in K^+ solutions occurs in a biphasic manner.

CD spectra of Tel22 G-quadruplexes in K^+ solutions monitored between 5 and 95 °C are characterized by a maximum at ∼293 nm, plateau at ∼265 nm, and minimum at ∼240 nm. It has been reported by several authors[31,37] that such spectra correspond to the hybrid type of G-quadruplexes (see Figure 2). Similarly, the corresponding DSC thermograms measured at three different concentrations of K^+ ions are characterized by two peaks whose position and height depend significantly on the K^+ concentration (Figure 3a). They clearly show that the thermal stability of Tel22 G-quadruplexes increases with increasing concentration of K^+ ions. This effect can be ascribed to stronger K^+-electrostatic screening of the negatively charged phosphate groups forming the DNA backbone. Since the observed DSC peaks indicate at least two thermally induced structural transitions and since PAGE shows no presence of higher G-quadruplex aggregates (see Figure S1 of the SI), we propose as the simplest possible model able to describe thermal unfolding of Tel22 the one presented in Figure 1. It assumes a temperature and K^+ concentration
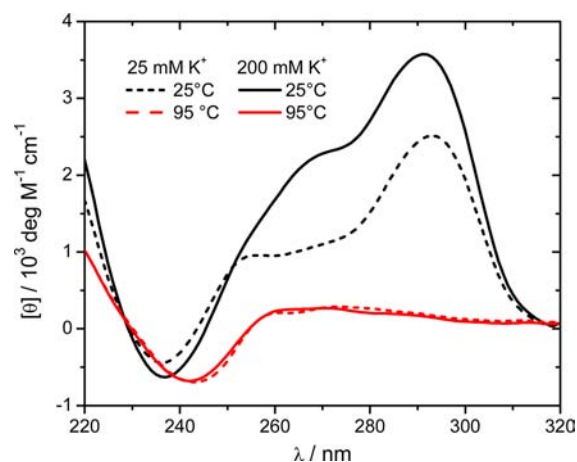
Figure 2. CD spectra of G-quadruplexes at 25 and 95 °C in the presence of 25 and 200 mM K^+ in cacodylic buffer, pH = 6.9.

dependent coexistence of three Tel22 distinguishable structural forms.

Accordingly, the state of a DNA solution of given structural composition at the temperature T and the concentration of K^+ ions c_{K^+}, contained in the sample cell of the applied instrument, can be defined in terms of the corresponding thermodynamic state function enthalpy, H_m, expressed per mol of DNA. For our experimental conditions at which $c_{K^+} \gg c_{DNA}$ the quantity H_m can be expressed as follows:

$$H_m = H_{m,b} + r\bar{H}_{KCl} + \bar{H}_2$$
$$= H_{m,b} + r\bar{H}_{KCl} + \alpha_F\bar{H}_F + \alpha_I\bar{H}_I + \alpha_U\bar{H}_U \quad (1)$$

where $H_{m,b}$ represents the enthalpy of buffer solution expressed per mol of DNA, $\bar{H}_2$ the partial molar enthalpy of DNA, $\bar{H}_{KCl}$ the partial molar enthalpy of added KCl, r the molar ratio KCl/DNA, $\bar{H}_i$ the partial molar enthalpy of the DNA species i (i = F, I, U), and α_i the molar ratio i/DNA ($\alpha_F + \alpha_I + \alpha_U = 1$). In the DSC experiments, the measured quantity is the temperature derivative of $\bar{H}_2$ (taken at constant pressure, buffer composition, KCl concentration and c_{DNA}), or in other words, the partial molar heat capacity of DNA, $\bar{C}_{P,2}$.[38] Similarly, the temperature derivative of $\bar{H}_i$ is the partial molar heat capacity of the species i, $\bar{C}_{P,i}$. Upon further analysis, $\bar{C}_{P,2}$ is more conveniently expressed as the excess heat capacity, $\Delta C_P = \bar{C}_{P,2} - \bar{C}_{P,int}$, where $\bar{C}_{P,int}$ represents an intrinsic heat capacity of DNA formally defined as $\bar{C}_{P,int} = \alpha_F\bar{C}_{P,F} + \alpha_I\bar{C}_{P,I} + \alpha_U\bar{C}_{P,U}$. In the measured temperature interval, $\bar{C}_{P,int}$ was approximated by the second order polynomial on T, fitted to the low-temperature (folded form) and high-temperature (unfolded form) parts of the experimental $\bar{C}_{P,2}$, and then subtracted from $\bar{C}_{P,2}$ to obtain ΔC_P (see Figure S3 of the SI). The excess heat capacity can also be calculated for the suggested model from the temperature derivative of eq 1 at constant pressure P. Since conformational transitions were followed experimentally at low concentrations, all $\bar{C}_{P,i}$, $\Delta C_{P,ij}$, $\bar{H}_i$, and ΔH_{ij} quantities appearing in the resulting model function may be replaced by their standard-state values, $\bar{C}^°_{P,i}$, $\Delta C^°_{P,ij}$, $\bar{H}^°_i$ and $\Delta H^°_{ij}$, and thus the model function for the excess heat capacity, ΔC_P, becomes:

$$\Delta C_P = (\partial\alpha_I/\partial T)\Delta H^°_{FI(T)} + (\partial\alpha_U/\partial T)\Delta H^°_{FU(T)} \quad (2)$$

where $\Delta H^°_{FI(T)} = \bar{H}^°_{I(T)} - \bar{H}^°_{F(T)}$ and $\Delta H^°_{FU(T)} = \bar{H}^°_{U(T)} - \bar{H}^°_{F(T)}$ are the standard enthalpies of interconversion of F to I and unfolding of F to U, respectively.
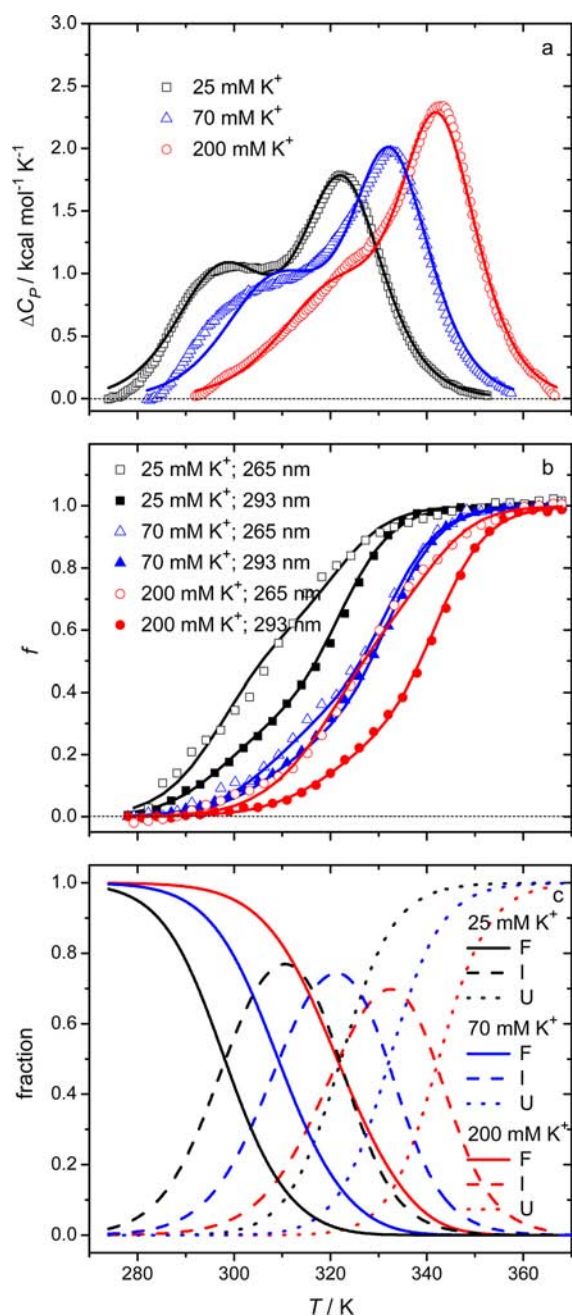
Figure 3. Global analysis of the DSC thermograms and CD melting curves measured at different concentrations of K^+ ions in cacodylic buffer, pH = 6.9: (a) DSC thermograms of Tel22 at different K^+ concentrations. Experimental data are presented by symbols, while the lines refer to the corresponding best global fit of the model function (eq 2). For clarity, only every fifth point is shown. (b) Normalized CD melting curves at 265 and 293 nm. Experimental data are presented by symbols while the corresponding best global fit of the model function (eq 4) is presented by the lines. (c) The model-based fractions of species F, I, and U as a function of T at different concentrations of K^+ ions determined using the "best fit" parameters reported in Table 1.

The measured CD spectra may be described in a similar way. According to the suggested model (Figure 1), the measured ellipticity at given wavelength corrected for the corresponding buffer contribution normalized to 1 M DNA and l = 1 cm, $[\theta]$, can be expressed as follows:

$$[\theta] = \alpha_F[\theta]_F + \alpha_I[\theta]_I + \alpha_U[\theta]_U \qquad (3)$$

where $[\theta]_i$ are the corresponding molar ellipticities of pure DNA conformations i at a given wavelength. By taking into account that $\alpha_F = 1 - \alpha_I - \alpha_U$ one obtains from eq 3 an expression for the normalized CD signal:[38]

$$f = \frac{[\theta] - [\theta]_F}{[\theta]_U - [\theta]_F} = \alpha_I f_{FI} + \alpha_U \qquad (4)$$

in which $[\theta]_F$ and $[\theta]_U$ values are obtained as pretransitional (low T) and post-transitional (high T) baselines linearly extrapolated over the whole measured T range. In eq 4, $f_{FI} = ([\theta]_I - [\theta]_F)/([\theta]_U - [\theta]_F)$ is considered as a temperature independent normalization coefficient, which was treated in the model analysis as an adjustable parameter.

According to the DSC- and CD-based model functions resulting from the suggested model (eqs 2 and 4) the thermodynamics of the proposed folding/unfolding mechanism (Figure 1) can be described by a set of adjustable parameters. Each transition step ij in this process is described in terms of the corresponding changes of three standard thermodynamic parameters that are independent of the K^+ concentration. Two of them, $\Delta G^\circ_{ij(T_0)}$ and $\Delta H^\circ_{ij(T_0)}$, depend on temperature and are thus determined at the reference temperature T_0 = 298.15 K, while the third parameter, $\Delta C^\circ_{P,ij}$ is assumed to be temperature independent. These three parameters define the standard free energy and enthalpy of transition, $\Delta G^\circ_{ij(T)}$ and $\Delta H^\circ_{ij(T)}$, at any T through the Gibbs−Helmholtz relation $[\partial(\Delta G^\circ_{ij(T)}/T)/\partial T]_P = -\Delta H^\circ_{ij(T)}/T^2$ and the Kirchhoff's law $[\partial\Delta H^\circ_{ij(T)}/\partial T]_P = \Delta C^\circ_{P,ij}$. Usually, each conformational transition is described in terms of the apparent $\Delta G^\circ_{ij(T,K^+)}$, which depends on K^+ concentration and considers the transition step as a process in which no release or uptake of counterions takes place. Its relation with the true thermodynamic $\Delta G^\circ_{ij(T)}$ which does not depend on K^+ concentration is given by the following:[38]

$$\Delta G^\circ_{ij(T,K^+)} = \Delta G^\circ_{ij(T)} + n_{ij}RT\ln[K^+]$$
$$= \Delta G^\circ_{ij(T_0)}T/T_0 + \Delta H^\circ_{ij(T_0)}[1 - T/T_0]$$
$$+ \Delta C^\circ_{P,ij}[T - T_0 - T\ln(T/T_0)]$$
$$+ n_{ij}RT\ln[K^+] \qquad (5)$$

where n_{ij} is the number of K^+ ions released or uptaken in the transition step ij and is assumed to be independent of T. Note that equilibrium concentration of unbound K^+, $[K^+]$, appearing in eq 5 is normalized to 1 M concentration in the reference state. Four thermodynamic parameters ($\Delta G^\circ_{ij(T_0)}$, $\Delta H^\circ_{ij(T_0)}$, $\Delta C^\circ_{P,ij}$, n_{ij} for ij = FI, IU) define each equilibrium constant, $K_{ij(T,K^+)} = \exp(-\Delta G^\circ_{ij(T,K^+)}/RT)$, appearing in the proposed model presented in Figure 1. In other words, eight parameters specify the populations of species F, I and U in the solution at any T and K^+ concentration ($K_{ij(T,K^+)} = f(\alpha_{i(T,K^+)}; i = F, I, U)$, $\sum_i \alpha_{i(T,K^+)} = 1 \Rightarrow \alpha_{i(T,K^+)} \Rightarrow (\partial\alpha_{i(T,K^+)}/\partial T)$) and consequently also the corresponding DSC and CD model functions (right-hand side of eqs 2 and 4). Global fitting of the model functions to the experimental DSC (Figure 3a) and CD (Figure 3b) data, measured at different K^+ concentrations, was based on the nonlinear Levenberg−Marquardt χ^2 regression procedure. The best-fit model functions show reasonably good agreement with the corresponding experimental data which may be considered as a sound support of the model presented in Figure 1. The

best-fit parameters obtained by the global analysis of DSC and CD data are presented in Table 1.

Table 1. Thermodynamic Parameters of Tel22 Unfolding in the Presence of K⁺ Ions at T_0 = 298.15 K Obtained by the Global Analysis of DSC and CD Data (eqs 2, 4) Based on the Three-State Model (Figure 1)^a

		F → I	I → U	F → U
$\Delta G^\circ_{ij(T_0)}$ (kcal mol⁻¹)		3.4 ± 0.2	6.2 ± 0.3	9.6 ± 0.5
$\Delta H^\circ_{ij(T_0)}$ (kcal mol⁻¹)		26.7 ± 1.0	28.8 ± 0.2	55.5 ± 1.2
$T\Delta S^\circ_{ij(T_0)}$ (kcal mol⁻¹)		23.3 ± 1.2	22.6 ± 0.5	45.9 ± 1.7
$\Delta C^\circ_{P,ij}$ (cal mol⁻¹ K⁻¹)		−20 ± 20	330 ± 30	310 ± 50
n_{ij}		1.5 ± 0.1	1.7 ± 0.1	3.2 ± 0.2
$T_{m,ij}$/°C^b	25 mM K⁺	25.1 ± 0.2	48.8 ± 0.2	38.1 ± 0.3
	70 mM K⁺	36.3 ± 0.8	59.0 ± 0.2	49.4 ± 0.2
	200 mM K⁺	48.4 ± 0.5	69.0 ± 0.2	60.8 ± 0.2

^{a}Standard deviations were obtained from diagonal elements of the corresponding variance-covariance matrix. $^b T_{m,ij}$ is the melting temperature defined as T at which $\alpha_i = \alpha_j$.

Interconversion Followed by ITC. Thermodynamics of the model-predicted interconversion of the intermediate form I into the folded form F upon increasing the K⁺ concentration was additionally checked by ITC. When monitored by ITC, the enthalpy changes, ΔH_T, resulting from the measured conformational transitions can be followed as $\Delta H_T = \Delta H - \Delta H_0$, where ΔH and ΔH_0 are the observed enthalpy changes accompanying the addition of KCl to the sample and blank (buffer) solution, respectively. In our experiments, the Tel22 G-quadruplex sample was prepared in a buffer solution with K⁺ concentration of c_{K^+} = 8 mM and titrated at 5 °C with 40 mM KCl dissolved in the same buffer solution to reach a final $c_{K^+} \approx$ 16 mM. Under these conditions, the thermodynamic analysis of the unfolding process (Table 1) predicts only the interconversion of I to F (Figure 4). Thus, the observed experimental enthalpy change, ΔH_T, can be described in terms of the model function that corresponds to the I → F interconversion and can be easily obtained from eq 1 by taking the partial derivative of $\bar{H}_2$ on r at $\alpha_U = 0$ and constant T, P, buffer composition, and c_{DNA}.[39,40]

$$\Delta H_T = (\partial \alpha_I / \partial r)\Delta H^\circ_{FI(T)} \tag{6}$$

$\Delta H^\circ_{FI(T)}$ appearing in eq 6 is the standard enthalpy of interconversion of F to I (see eq 2) and r is the added K⁺/DNA molar ratio. The value of the model function was calculated at each r using the model-based thermodynamic values ($\Delta H^\circ_{FI(T)}$, $\Delta G^\circ_{FI(T)}$) obtained for Tel22 unfolding followed by DSC and CD (Table 1). To obtain optimum agreement between experimental and calculated titration curves the number of K⁺ ions released upon F → I transition, n_{FI}, was used as a fitting parameter. The resulting "best fit" value of n_{FI} = 1.3 differs slightly from the value of n_{FI} = 1.5 obtained from the global fitting of the DSC and CD melting curves (Table 1). Considering that calorimetric titrations were performed at substantially lower K⁺ concentration than DSC and CD melting experiments, we believe that the agreement between the two n_{FI} values is reasonably good and thus fully supports our model (Figure 1).

Mechanism and Driving Forces of Folding/Unfolding. As shown in Table 1, the described model-based analysis of the experimental DSC and CD data leads to the conclusion that the F → U overall unfolding of Tel22 is accompanied by a
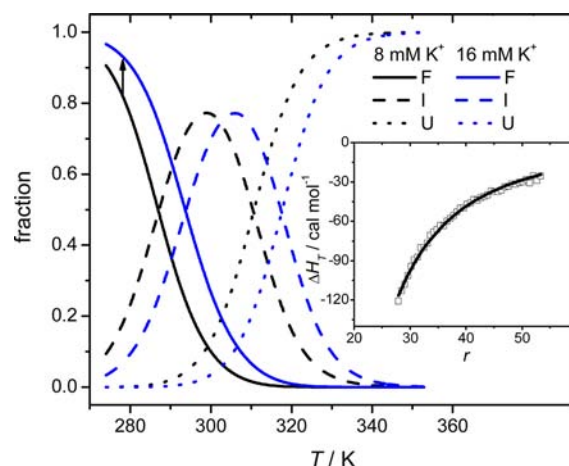
Figure 4. Model (see Figure 1) predicted fractions of species F, I, and U at the beginning (8 mM K⁺) and at the end (16 mM K⁺) of the ITC experiment. Experiment was performed at 5 °C by titrating $c_{DNA} \approx$ 0.3 mM G-quadruplex solution in TRIS buffer, pH = 6.9 with c_s = 40 mM KCl solution in the same buffer. Inset: Enthalpy of interconversion of I into F resulting from KCl to DNA titration as a function of K⁺/DNA molar ratio r is represented by symbols. The corresponding model function represented by the line (eq 6) was calculated from the data presented in Table 1 with only the number of associated ions, n_{FI}, used as a fitting parameter.

substantial positive heat capacity change ($\Delta C^\circ_{P,FU}$ = 310 ± 50 cal mol⁻¹ K⁻¹). This result is consistent with the positive ΔC_P effects observed with helix-to-coil transitions of DNA duplexes[41−43] and agrees well with the DSC-based ΔC_P value of 155−192 cal mol⁻¹ K⁻¹ reported for the unfolding of the two G-quartets containing 5′-GGTTGGTGTGGTTGG-3′ quadruplex in 100 mM KCl[44] and with the ΔC_P of unfolding of Tel22 of 401 cal mol⁻¹ K⁻¹ computed on the basis of the accompanying changes in exposure of its polar and nonpolar surface area.[45] Moreover, the overall enthalpy change accompanying the F → U unfolding process is equal to 55.5 kcal per mole of Tel22 or 18.5 kcal per mole of G-quartets, a value that agrees well with the corresponding literature data.[10,27,46] Finally, as shown in Table 1, the overall F → U unfolding is characterized by an extensive enthalpy−entropy compensation resulting in a relatively small $\Delta G^\circ_{ij(T_0)}$ value.

A detailed model-based global thermodynamic analysis of DSC and CD data shows that the fractions of the folded, intermediate, and unfolded structures present in the solution depend on T and K⁺ concentration (Figure 3c). Analysis of DSC and CD data obtained at different K⁺ concentrations allowed us to estimate the overall number of K⁺ ions released upon unfolding of the most stable G-quadruplex structure F into single strands; n_{FU} = 3.2 (eq 5, Table 1). According to the recent structural information on Tel22 topology the most stable Tel22 G-quadruplex structure at low temperatures could be a mixture of two hybrid structures, Hybrid-1 and Hybrid-2. With increasing temperature, these structures first unfold into the corresponding triplex structures and then into the fully extended state.[34] Assuming that the DSC, CD, and ITC techniques cannot distinguish between the two energetically very similar hybrid quadruplex or triplex structures, one can expect that according to our measurements the hybrid mixture will appear as a single thermodynamic state F and the triplex mixture as a single thermodynamic state I. As suggested by Chaires et al.[33] in their molecular dynamics study on structural

topology of Tel22 in K^+ solutions the Hybrid-1 contains three specific binding sites for K^+ ions (two channel sites and one external site) while the Hybrid-2 structure is stabilized by only two K^+ ions (two channel sites). In other words, upon unfolding of Tel22 native state 2–3 specifically bound K^+ ions are released. We believe that this structure-based prediction is in good agreement with the corresponding thermodynamic value of $n_{FU} = 3.2$ obtained in this work, especially since n_{FU} includes the ions bound specifically (quadruplex channels, external site) together with the difference of ions condensed (electrostatically bound) on the G-quadruplex and on its unfolded form.

As suggested in Figure 1, the thermally induced unfolding of Tel22 involves both, the stepwise transition of structure F into a less stable (intermediate) structure I followed by a transition into the unfolded single stranded structure U and the straightforward transition F → U. The F → I transition is characterized by: (a) changes in enthalpy and entropy equal to about half of their values for the overall F → U transition, $\Delta H^{\circ}_{FI(T_0)} \approx 1/2\Delta H^{\circ}_{FU(T_0)}$ and $T\Delta S^{\circ}_{FI(T_0)} \approx 1/2T\Delta S^{\circ}_{FU(T_0)}$, (b) almost negligible change in heat capacity, $\Delta C^{\circ}_{P,FI} = -20 \pm 20$ cal mol^{-1} K^{-1} and (c) a release of K^+ ions, $n_{FI} = 1.5$, significantly lower than the overall release, n_{FU} (Table 1). These changes are consistent with the already mentioned structural model of the Tel22 unfolding mechanism[34] which considers Tel22 unfolding as a two-step process. In the first step, which corresponds to the F → I transition in our model, the Hybrid-1 and Hybrid-2 G-quadruplexes undergo transitions into the corresponding triplex structures which contain only one specifically bound K^+ ion and are characterized by water-exposed G-rich 3′ and 5′ ends of the partially unfolded hybrid structures. Thus, the first step is expected to be accompanied by a release of 1–2 specifically bound K^+ ions and by a substantial positive enthalpy and entropy of transition. Moreover, the compensation of the ΔC_P contributions due to the simultaneous exposure of hydrophobic parts (deoxyribose) to water with accompanying $\Delta C_P > 0$ effect and the release of K^+ ions together with the exposure of polar parts (guanine, phosphate) with accompanying $\Delta C_P < 0$ contribution should result in a small overall ΔC_P of transition.[47–49] Similar consistency is observed also between our results for the I → U transition ($\Delta H^{\circ}_{IU(T_0)} \approx 1/2\Delta H^{\circ}_{FU(T_0)}$ and $T\Delta S^{\circ}_{IU(T_0)} \approx 1/2T\Delta S^{\circ}_{FU(T_0)}$, $\Delta C^{\circ}_{P,IU} = 330 \pm 30$ cal mol^{-1} K^{-1}, $n_{IU} = 1.7$) and the predictions of the structural model for the corresponding second step in which the triplex structures undergo a transition into the unfolded form. Considering that triplex structures contain one specifically bound K^+ ion and that upon unfolding some of the condensed K^+ ions are released one can expect that this transition will be accompanied by a release of more than one K^+ ion. In addition, unfolding of triplex structures should be accompanied with substantial positive enthalpy and entropy of transition and, due to the unfolding-induced exposure of a large number of thymines and other hydrophobic groups to water with a substantial positive change in heat capacity.[47]

In conclusion, our thermodynamic model of Tel22 folding/unfolding transitions and its characterization through the accompanying changes in enthalpy, entropy, heat capacity, and the number of released K^+ ions can be reasonably well explained only if the model-predicted intermediate state participating in the overall folding/unfolding process is considered to be a partially unfolded quadruplex; a triplex conformation. This characterization enables us to predict the

populations of Tel22 conformations in solution in a wide temperature and K^+ concentration range (Figure 5). We are
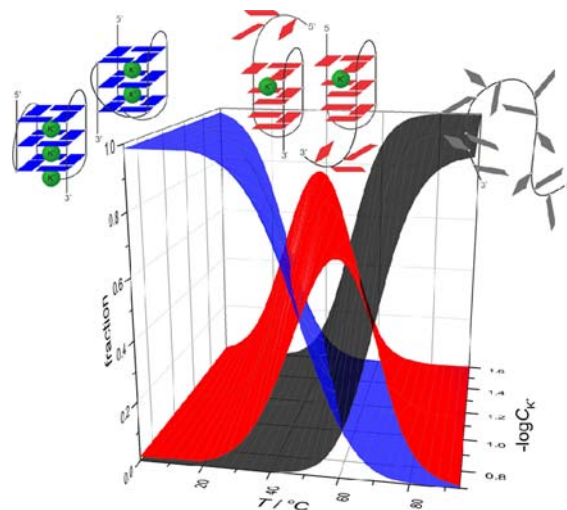
Figure 5. Predicted populations of Tel22 conformations in solution as a function of temperature and K^+ concentration. From left to right: the suggested Hybrid-1, Hybrid-2 (blue), Triplex-1, Triplex-2 (red), and unfolded single-stranded form (gray).[33,34]

aware of the fact that the reported theoretical study on Tel22 unfolding transitions[34] provides no information on whether the predicted intermediate triplex conformations are stable or not. Our results, however, clearly demonstrate that in the thermal unfolding of Tel22 a stable intermediate state is involved and that the corresponding thermodynamic quantities of transition can be well explained in terms of the theoretically predicted unfolding pathways. Therefore, we believe that the results of our work represent the first experimental support of the recently suggested folding/unfolding mechanism of Tel22 that predicts its unfolding transitions via intermediate triplex conformations.

■ ASSOCIATED CONTENT

Ⓢ Supporting Information
PAGE electrophoresis experiments, normalized CD and UV melting curves at different DNA concentrations and analysis of DSC thermograms; from $\bar{C}_{P,2}$ values to ΔC_P. This material is available free of charge via the Internet at http://pubs.acs.org.

■ AUTHOR INFORMATION

Corresponding Author
jurij.lah@fkkt.uni-lj.si; gorazd.vesnaver@fkkt.uni-lj.si
Notes
The authors declare no competing financial interest.

■ ACKNOWLEDGMENTS

■ REFERENCES

(1) Gellert, M.; Lipsett, M. N.; Davies, D. R. *Proc. Natl. Acad. Sci. U.S.A.* **1962**, *48*, 2013−2018.

(2) Neidle, S.; Balasubramanian, S. *Quadruplex Nucleic Acids*; RSC Publishing, Cambridge, UK, 2006.

(3) Burge, S.; Parkinson, G. N.; Hazel, P.; Todd, A. K.; Neidle, S. *Nucleic Acids Res.* **2006**, *34*, 5402−5415.

(4) Webba da Silva, M. *Chemistry* **2007**, *13*, 9738−9745.

(5) Webba da Silva, M.; Trajkovski, M.; Sannohe, Y.; Ma'ani Hessari, N.; Sugiyama, H.; Plavec, J. *Angew. Chem., Int. Ed.* **2009**, *48*, 9167−9170.

(6) Črnugelj, M.; Šket, P.; Plavec, J. *J. Am. Chem. Soc.* **2003**, *125*, 7866−7871.

(7) Šket, P.; Plavec, J. *J. Am. Chem. Soc.* **2010**, *132*, 12724−12732.

(8) Zhang, Z.; Dai, J.; Veliath, E.; Jones, R. A.; Yang, D. *Nucleic Acids Res.* **2009**, *38*, 1009−1021.

(9) Lee, J. Y.; Okumus, B.; Kim, D. S.; Ha, T. *Proc. Natl. Acad. Sci. U.S.A.* **2005**, *102*, 18938−18943.

(10) Prislan, I.; Lah, J.; Vesnaver, G. *J. Am. Chem. Soc.* **2008**, *130*, 14161−14169.

(11) Prislan, I.; Lah, J.; Milanic, M.; Vesnaver, G. *Nucleic Acids Res.* **2011**, *39*, 1933−1942.

(12) Olsen, C. M.; Gmeiner, W. H.; Marky, L. A. *J. Phys. Chem. B* **2006**, *110*, 6962−6969.

(13) Dai, J.; Carver, M.; Punchihewa, C.; Jones, R. A.; Yang, D. *Nucleic Acids Res.* **2007**, *35*, 4927−4940.

(14) Ambrus, A.; Chen, D.; Dai, J.; Bialis, T.; Jones, R. A.; Yang, D. *Nucleic Acids Res.* **2006**, *34*, 2723−2735.

(15) Dai, J.; Punchihewa, C.; Ambrus, A.; Chen, D.; Jones, R. A.; Yang, D. *Nucleic Acids Res.* **2007**, *35*, 2440−2450.

(16) Zahler, A. M.; Williamson, J. R.; Cech, T. R.; Prescott, D. M. *Nature* **1991**, *350*, 718−720.

(17) Neidle, S.; Parkinson, G. *Nat. Rev. Drug. Discov.* **2002**, *1*, 383−393.

(18) Neidle, S. *FEBS Lett.* **2010**, *277*, 1118−1125.

(19) Sun, D.; Thompson, B.; Cathers, B. E.; Salazar, M.; Kerwin, S. M.; Trent, J. O.; Jenkins, T. C.; Neidle, S.; Hurley, L. H. *J. Med. Chem.* **1997**, *40*, 2113−3116.

(20) Balasubramanian, S.; Hurley, L. H.; Neidle, S. *Nat. Rev. Drug Discovery* **2011**, *10*, 261−275.

(21) Monchaud, D.; Teulade-Fichou, M. P. *Org. Biomol. Chem.* **2008**, *6*, 627−636.

(22) De Cian, A.; DeLemos, E.; Mergny, J. L.; Teulade-Fichou, M. P.; Monchaud, D. *J. Am. Chem. Soc.* **2007**, *129*, 1856−1857.

(23) Dixon, I. M.; Lopez, F.; Tejera, A. M.; Estève, J. P.; Blasco, M. A.; Pratviel, G.; Meunier, B. *J. Am. Chem. Soc.* **2007**, *129*, 1502−1503.

(24) Hamon, F.; Largy, E.; Guédin-Beaurepaire, A.; Rouchon-Dagois, M.; Sidibe, A.; Monchaud, D.; Mergny, J. L.; Riou, J. F.; Nguyen, C. H.; Teulade-Fichou, M. P. *Angew. Chem., Int. Ed.* **2011**, *50*, 8745−8749.

(25) Antonacci, C.; Chaires, J. B.; Sheardy, R. D. *Biochemistry* **2007**, *46*, 4654−4660.

(26) Gray, R. D.; Li, J.; Chaires, J. B. *J. Phys. Chem. B* **2009**, *113*, 2676−2683.

(27) Mergny, J. L.; Phan, A. T.; Lacroix, L. *FEBS Lett.* **1998**, *435*, 74−78.

(28) Parkinson, G. N.; Lee, M. P. H.; Neidle, S. *Nature* **2002**, *417*, 876−880.

(29) Wang, Y.; Patel, D. J. *Structure* **1993**, *1*, 263−282.

(30) Li, J.; Correia, J. J.; Wang, L.; Trent, J. O.; Chaires, J. B. *Nucleic Acids Res.* **2005**, *14*, 4649−4659.

(31) Xu, Y.; Noguchi, Y.; Sugiyama, H. *Bioorgan. Med. Chem.* **2006**, *14*, 5584−5591.

(32) Phan, A. T.; Kuryavyi, V.; Luu, K. N.; Patel, D. J. *Nucleic Acids Res.* **2007**, *35*, 6517−6525.

(33) Gray, R. D.; Petraccone, L.; Trent, J. O.; Chaires, J. B. *Biochemistry* **2010**, *49*, 179−194.

(34) Mashimo, T.; Yagi, H.; Sannohe, Y.; Rajendran, A.; Sugiyama, H. *J. Am. Chem. Soc.* **2010**, *132*, 14910−14918.

(35) Cantor, C. R.; Warshaw, M. M.; Shapiro, H. *Biopolymers* **1970**, *9*, 1059−1077.

(36) Lah, J.; Drobnak, I.; Dolinar, I.; Vesnaver, G. *Nucleic Acids Res.* **2008**, *30*, 897−904.

(37) Rentčiuk, D.; Kejnovská, I.; Školáková, P.; Bednářová, K.; Motlová, J.; Vorličková, M. *Nucleic Acids Res.* **2009**, *37*, 6625−6634.

(38) Drobnak, I.; Vesnaver, G.; Lah, J. *J. Phys. Chem. B* **2010**, *114*, 8713−8722.

(39) Lah, J.; Maier, N. M.; Lindner, W.; Vesnaver, G. *J. Phys. Chem. B* **2001**, *105*, 1670−1678.

(40) Lah, J.; Vesnaver, G. *Croat. Chem. Acta* **2001**, *74*, 37−49.

(41) Tikhomirova, A.; Taulier, N.; Chalikian, T. V. *J. Am. Chem. Soc.* **2004**, *126*, 16387−16394.

(42) Drobnak, I.; Seručnik, M.; Lah, J.; Vesnaver, G. *Acta Chim. Slov.* **2007**, *54*, 445−451.

(43) Chalikian, T. V.; Volker, J.; Plum, G. E.; Breslauer, K. J. *Proc. Natl. Acad. Sci. U.S.A.* **1999**, *96*, 7853−7858.

(44) Smirnov, I.; Shafer, R. H. *Biochemistry* **2000**, *39*, 1462−1468.

(45) Majhi, P. R.; Qi, J.; Tang, C.-F.; Shafer, R. H. *Biopolymers* **2008**, *89*, 302−309.

(46) Jin, R.; Gaffney, B. L.; Wang, C.; Jones, R. A.; Breslauer, K. J. *Proc. Natl. Acad. Sci. U.S.A.* **1992**, *89*, 8832−8836.

(47) Madan, B.; Sharp, K. A. *Biophys. J.* **2001**, *81*, 1881−1887.

(48) Olsen, C. M.; Marky, L. A. *J. Phys. Chem. B* **2009**, *113*, 9−11.

(49) Cullis, P. M.; Wolfenden, R. *Biochemistry* **1981**, *20*, 3024−3028.

(50) Koirala, D.; Mashimo, T.; Sannohe, Y.; Yu, Z.; Mao, H.; Sugiyama, H. *Chem. Commun.* **2012**, *48*, 2006−2008.

■ NOTE ADDED IN PROOF

A paper on the intramolecular folding in three (Tel 3G) and four (Tel 4G) tandem guanine repeats of human telomeric DNA in Na$^+$ and K$^+$ solutions appeared online during the review of our paper. In this study, it has been demonstrated that folding of Tel 4G in K$^+$ solutions results in the coexistence of two mechanically and thermodynamically stable species; one is consistent with a triplex conformation, while the other has characteristics of a G quadruplex conformation.[50]